

A TREATMENT OF CONTACT DISCONTINUITY FOR CENTRAL UPWIND SCHEME BY CHANGING FLUX FUNCTIONS

MOUNGIN SHIN¹, SUYEON SHIN¹, AND WOONJAE HWANG^{2,†}

¹DEPARTMENT OF MATHEMATICS, KOREA UNIVERSITY, SEOUL, KOREA

E-mail address: {smopower, angelic52}@korea.ac.kr

²DEPARTMENT OF INFORMATION AND MATHEMATICS, KOREA UNIVERSITY, SEJONG, KOREA

E-mail address: woonjae@korea.ac.kr

ABSTRACT. Central schemes offer a simple and versatile approach for computing approximate solutions of nonlinear systems of hyperbolic conservation laws. However, there are large numerical dissipation in case of contact discontinuity. We study semi-discrete central upwind scheme by changing flux functions to reduce the numerical dissipation and we perform numerical computations for various problems in case of contact discontinuity.

1. INTRODUCTION

In this paper, we study second-order Godunov type central upwind scheme for one dimensional and two dimensional system of hyperbolic conservation laws. The first order central scheme was introduced by Lax Friedrichs [9]. However, there are large numerical dissipations. One dimensional second order central scheme was proposed by Nessyahu and Tadmor [12] and two dimensional second order central scheme was introduced by Jiang and Tadmor [2]. The central schemes for conservation laws has a lot of attentions since their simplicity and efficiency that does not require any Riemann Solvers and that have a smaller numerical dissipations than the first order Lax Friedrichs[7, 10, 11, 13]. Kugarnov and Tadmor [8] proposed a new class of central scheme that has a low numerical dissipations. After then, Kugarnov et al. [5] introduced a semi-discrete central upwind scheme which has a much smaller numerical dissipations by considering the one side local speed. Kurganov and Petrova [6] introduced a central upwind scheme that changes flux functions to reduce the numerical dissipations of contact discontinuity. Kurganov and Lin [4] proposed new semi discrete central upwind scheme to decrease a relatively large amount of numerical dissipation present at the staggered central schemes. In this paper, we only consider semi discrete type central upwind scheme. In sections

Received by the editors June 20 2012; Accepted February 4 2013.

2010 *Mathematics Subject Classification.* 35L65, 74S20.

Key words and phrases. contact discontinuity, central upwind scheme, flux function, conservation laws.

† Corresponding author.

This research was supported by Basic Science Research Programm through the National Research Foundation of Korea(NRF) funded by the Ministry of Education, Science and Technology(Grant No. 2010-0025523).

2 and 4, two different types of modified semi-discrete central upwind schemes (Modified CU1 and Modified CU2) are introduced to treat a numerical dissipations of contact discontinuity by changing flux function for one dimensional and two dimensional cases [4, 5, 6], respectively. In sections 3 and 5, we do numerical experiments for the various problems for one dimensional and two dimensional cases, respectively. We compare the numerical results of original semi discrete central upwind scheme(CU), Modified CU1 and Modified CU2.

2. ONE DIMENSIONAL SEMI-DISCRETE CENTRAL UPWIND SCHEME

In this section, we consider semi discrete central upwind scheme [5] for one dimensional system of hyperbolic conservation laws:

$$u_t + f(u)_x = 0. \quad (2.1)$$

We only consider uniform grids: $x_\alpha := \alpha \Delta x$, $t^\beta := \beta \Delta t$, $\lambda := \Delta t / \Delta x$. We also assume that at a certain time level the cell averages of the solution:

$$\bar{u}_j^n \approx \frac{1}{\Delta x} \int_{x_{j-\frac{1}{2}}}^{x_{j+\frac{1}{2}}} u(x, t^n) dx \quad (2.2)$$

are available. Using the cell averages \bar{u}_j^n we reconstruct a 2nd-order piecewise linear interpolation:

$$\tilde{u}(x, t^n) = \sum_j [\bar{u}_j^n + s_j^n(x - x_j)] \chi_j(x). \quad (2.3)$$

Here, s_j^n is slope of the corresponding linear pieces and $\chi_j(x)$ is the characteristic function over the cell $(x_{j-\frac{1}{2}}, x_{j+\frac{1}{2}})$. We take

$$s_j^n = \text{minmod}\left(\theta \frac{\bar{u}_{j+1}^n - \bar{u}_j^n}{\Delta x}, \frac{\bar{u}_{j+1}^n - \bar{u}_{j-1}^n}{2\Delta x}, \theta \frac{\bar{u}_j^n - \bar{u}_{j-1}^n}{\Delta x}\right), \theta \in [1, 2] \quad (2.4)$$

where the minmod function is defined as follows:

$$\text{minmod}(c_1, c_2, \dots, c_m) = \begin{cases} \min(c_1, c_2, \dots, c_m) & \text{if } c_i > 0 \quad \forall i = 1, \dots, m \\ \max(c_1, c_2, \dots, c_m) & \text{if } c_i < 0 \quad \forall i = 1, \dots, m \\ 0 & \text{otherwise.} \end{cases} \quad (2.5)$$

Upper bound on the right-side and left-side local speeds can be computed by

$$a_{j+\frac{1}{2}}^+ := \max_{\omega \in C(u_{j+\frac{1}{2}}^-, u_{j+\frac{1}{2}}^+)} \{\lambda_N(A(\omega)), 0\} \quad \text{and} \quad a_{j+\frac{1}{2}}^- := \min_{\omega \in C(u_{j+\frac{1}{2}}^-, u_{j+\frac{1}{2}}^+)} \{\lambda_1(A(\omega)), 0\},$$

respectively. Here, $\lambda_1 < \lambda_2 < \dots < \lambda_N$ are N eigenvalues of the corresponding Jacobians, $A := \frac{\partial f}{\partial u}$, and $C(u_{j+\frac{1}{2}}^-, u_{j+\frac{1}{2}}^+)$ is the curve in the phase space that connects the left state,

$$u_{j+\frac{1}{2}}^- := \bar{u}_j^n + \frac{\Delta x}{2} s_j^n,$$

and the right state,

$$u_{j+\frac{1}{2}}^+ := \bar{u}_{j+1}^n - \frac{\Delta x}{2} s_{j+1}^n.$$

In the case of convex flux f , the local speeds can be estimated as follows:

$$\begin{aligned} a_{j+\frac{1}{2}}^+ &:= \max\{\lambda_N(A(u_{j+\frac{1}{2}}^-)), \lambda_N(A(u_{j+\frac{1}{2}}^+)), 0\}, \\ a_{j+\frac{1}{2}}^- &:= \min\{\lambda_1(A(u_{j+\frac{1}{2}}^-)), \lambda_1(A(u_{j+\frac{1}{2}}^+)), 0\}. \end{aligned}$$

We consider the nonequal rectangular domains

$$[x_{j-\frac{1}{2},r}^n, x_{j+\frac{1}{2},l}^n] \times [t^n, t^{n+1}] \quad \text{and} \quad [x_{j+\frac{1}{2},l}^n, x_{j+\frac{1}{2},r}^n] \times [t^n, t^{n+1}] \quad (2.6)$$

with $x_{j+\frac{1}{2},l}^n := x_{j+\frac{1}{2}} + a_{j+\frac{1}{2}}^- \Delta t$ and $x_{j+\frac{1}{2},r}^n := x_{j+\frac{1}{2}} + a_{j+\frac{1}{2}}^+ \Delta t$. Then CFL condition is satisfied:

$$\Delta t \cdot \max_j \{\max(a_{j+\frac{1}{2}}^+, -a_{j+\frac{1}{2}}^-)\} < \frac{\Delta x}{2}.$$

By integrating (1) over nonequal rectangular domain with the midpoint approximation of the flux integrals, we obtain cell average at time $t = t^{n+1}$, over the non-smooth areas:

$$\begin{aligned} \bar{\omega}_{j+\frac{1}{2}}^{n+1} &= \frac{1}{a_{j+\frac{1}{2}}^+ - a_{j+\frac{1}{2}}^-} \left\{ u_{j+\frac{1}{2},r}^n a_{j+\frac{1}{2}}^+ - \frac{s_{j+1}^n}{2} (a_{j+\frac{1}{2}}^+)^2 \Delta t - u_{j+\frac{1}{2},l}^n a_{j+\frac{1}{2}}^- \right. \\ &\quad \left. + \frac{s_j^n}{2} (a_{j+\frac{1}{2}}^-)^2 \Delta t - \left[f(u_{j+\frac{1}{2},r}^{n+\frac{1}{2}}) - f(u_{j+\frac{1}{2},l}^{n+\frac{1}{2}}) \right] \right\} \end{aligned}$$

and, similarly, over the smooth areas:

$$\bar{\omega}_j^{n+1} = \bar{u}_j^n + \frac{s_j^n}{2} (a_{j+\frac{1}{2}}^+ + a_{j+\frac{1}{2}}^-) \Delta t - \frac{\Delta t}{\Delta x - (a_{j-\frac{1}{2}}^+ - a_{j+\frac{1}{2}}^-) \Delta t} \left[f(u_{j+\frac{1}{2},l}^{n+\frac{1}{2}}) - f(u_{j-\frac{1}{2},r}^{n+\frac{1}{2}}) \right].$$

The piecewise linear reconstructions are

$$u_{j+\frac{1}{2},l}^n := \bar{u}_j^n + s_j^n \left(\frac{\Delta x}{2} + a_{j+\frac{1}{2}}^- \Delta t \right) \quad \text{and} \quad u_{j+\frac{1}{2},r}^n := \bar{u}_{j+1}^n - s_{j+1}^n \left(\frac{\Delta x}{2} - a_{j+\frac{1}{2}}^+ \Delta t \right),$$

and the midpoint values are obtained from the corresponding Taylor expansions,

$$u_{j+\frac{1}{2},l}^{n+\frac{1}{2}} = u_{j+\frac{1}{2},l}^n - \frac{\Delta t}{2} f(u_{j+\frac{1}{2},l}^n)_x \quad \text{and} \quad u_{j+\frac{1}{2},r}^{n+\frac{1}{2}} = u_{j+\frac{1}{2},r}^n - \frac{\Delta t}{2} f(u_{j+\frac{1}{2},r}^n)_x.$$

We take a piecewise linear interpolant:

$$\begin{aligned} \tilde{\omega}(x, t^{n+1}) &:= \sum_j \left\{ \left[\bar{\omega}_{j+\frac{1}{2}}^{n+1} + s_{j+\frac{1}{2}}^{n+1} \left(x - \frac{x_{j+\frac{1}{2},l}^n + x_{j+\frac{1}{2},r}^n}{2} \right) \right] \chi_{[x_{j+\frac{1}{2},l}^n, x_{j+\frac{1}{2},r}^n]} \right. \\ &\quad \left. + \bar{\omega}_j^{n+1} \chi_{[x_{j-\frac{1}{2},r}^n, x_{j+\frac{1}{2},l}^n]} \right\} \end{aligned}$$

is reconstructed from the evolved intermediate cell averages $\{\bar{\omega}_{j+\frac{1}{2}}^{n+1}\}, \{\bar{\omega}_j^{n+1}\}$. This results in the new projected cell average:

$$\begin{aligned} \bar{u}_j^{n+1} &= \lambda a_{j-\frac{1}{2}}^+ \bar{\omega}_{j-\frac{1}{2}}^{n+1} + [1 + \lambda(a_{j-\frac{1}{2}}^- - a_{j+\frac{1}{2}}^+)] \bar{\omega}_j^{n+1} - \lambda a_{j+\frac{1}{2}}^- \bar{\omega}_{j+\frac{1}{2}}^{n+1} \\ &\quad + \frac{\lambda \Delta t}{2} [s_{j+\frac{1}{2}}^{n+1} a_{j+\frac{1}{2}}^+ a_{j+\frac{1}{2}}^- - s_{j-\frac{1}{2}}^{n+1} a_{j-\frac{1}{2}}^+ a_{j-\frac{1}{2}}^-]. \end{aligned} \quad (2.7)$$

From (7) we obtain that

$$\begin{aligned} \frac{d}{dt} \bar{u}_j(t) &= \lim_{\Delta t \rightarrow 0} \frac{\bar{u}_j^{n+1} - \bar{u}_j^n}{\Delta t} \\ &= \frac{a_{j-\frac{1}{2}}^+}{\Delta x} \lim_{\Delta t \rightarrow 0} \bar{\omega}_{j-\frac{1}{2}}^{n+1} + \lim_{\Delta t \rightarrow 0} \frac{1}{\Delta t} \{[1 + \lambda(a_{j-\frac{1}{2}}^- - a_{j+\frac{1}{2}}^+)] \bar{\omega}_j^{n+1} - \bar{u}_j^n\} \\ &\quad - \frac{a_{j+\frac{1}{2}}^-}{\Delta x} \lim_{\Delta t \rightarrow 0} \bar{\omega}_{j+\frac{1}{2}}^{n+1} + \frac{1}{2\Delta x} \lim_{\Delta t \rightarrow 0} \left[\Delta t \left(s_{j+\frac{1}{2}}^{n+1} a_{j+\frac{1}{2}}^+ a_{j+\frac{1}{2}}^- - s_{j-\frac{1}{2}}^{n+1} a_{j-\frac{1}{2}}^+ a_{j-\frac{1}{2}}^- \right) \right]. \end{aligned} \quad (2.8)$$

One-dimensional semi-discrete central upwind scheme which can be written in the conservative form is

$$\frac{d}{dt} \bar{u}_j(t) = -\frac{H_{j+\frac{1}{2}}(t) - H_{j-\frac{1}{2}}(t)}{\Delta x},$$

with the numerical flux $H_{j+\frac{1}{2}}$, given by

$$\begin{aligned} H_{j+\frac{1}{2}}(t) &:= \frac{a_{j+\frac{1}{2}}^+ f(u_{j+\frac{1}{2}}^-) - a_{j+\frac{1}{2}}^- f(u_{j+\frac{1}{2}}^+)}{a_{j+\frac{1}{2}}^+ - a_{j+\frac{1}{2}}^-} + \frac{a_{j+\frac{1}{2}}^+ a_{j+\frac{1}{2}}^-}{a_{j+\frac{1}{2}}^+ - a_{j+\frac{1}{2}}^-} [u_{j+\frac{1}{2}}^+ - u_{j+\frac{1}{2}}^-] \\ &\quad - \frac{a_{j+\frac{1}{2}}^+ a_{j+\frac{1}{2}}^-}{2} \lim_{\Delta t \rightarrow 0} (\Delta t s_{j+\frac{1}{2}}^{n+1}). \end{aligned} \quad (2.9)$$

The second order Runge-Kutta method is applied for time evolution.

2.1. Modified CU1[6]. The slope $s_{j+\frac{1}{2}}^{n+1}$ in (9) is to be evaluated. It can be done by several different ways. For example, the component-wise approach was implemented in [6]. The slope is computed by

$$\begin{aligned} s_{j+\frac{1}{2}}^{n+1} &= \\ 2 \cdot \text{minmod} \left(\theta \frac{\bar{\omega}_{j+\frac{1}{2}}^{n+1} - \bar{\omega}_j^{n+1}}{x_{j+\frac{1}{2},r}^n - x_{j-\frac{1}{2},r}^n}, \frac{\bar{\omega}_{j+1}^{n+1} - \bar{\omega}_j^{n+1}}{x_{j+\frac{3}{2},l}^n - x_{j+\frac{1}{2},l}^n + x_{j+\frac{1}{2},r}^n - x_{j-\frac{1}{2},r}^n}, \theta \frac{\bar{\omega}_{j+1}^{n+1} - \bar{\omega}_{j+\frac{1}{2}}^{n+1}}{x_{j+\frac{3}{2},l}^n - x_{j+\frac{1}{2},l}^n} \right). \end{aligned} \quad (2.10)$$

Figure 1 shows that how we can compute slope using (10). In Figure 1, the slope $s_{j+\frac{1}{2}}^{n+1}$ of Modified CU1 is the smallest one from three slopes which is computed in (10) by using the

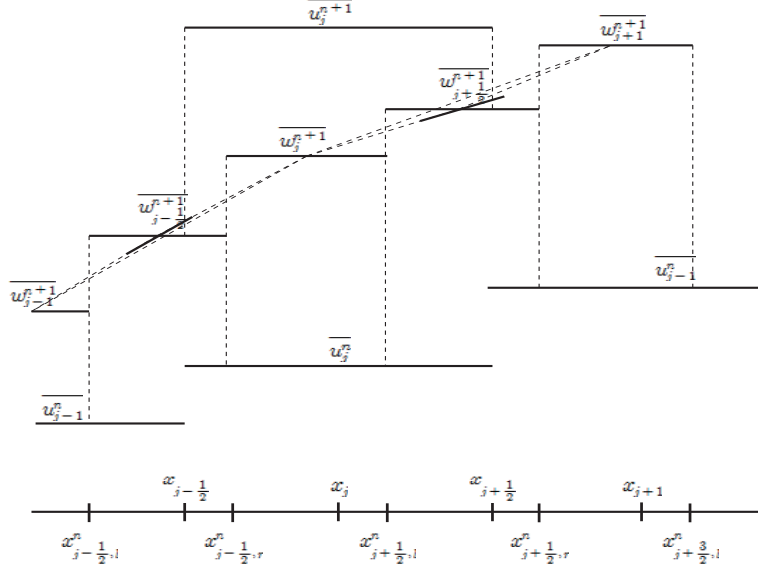


FIGURE 1. Modified CU1

values \bar{w}_j^{n+1} , $\bar{w}_{j+\frac{1}{2}}^{n+1}$, and \bar{w}_{j+1}^{n+1} . Here, the distances are

$$x_{j+\frac{1}{2},r}^n - x_{j-\frac{1}{2},r}^n = \Delta x + \Delta t(a_{j+\frac{1}{2}}^+ - a_{j-\frac{1}{2}}^-), \quad x_{j+\frac{3}{2},l}^n - x_{j+\frac{1}{2},l}^n = \Delta x + \Delta t(a_{j+\frac{3}{2}}^- - a_{j+\frac{1}{2}}^-).$$

Then we can evaluate $\lim_{\Delta t \rightarrow 0} (\Delta t s_{j+\frac{1}{2}}^{n+1})$ by

$$\lim_{\Delta t \rightarrow 0} (\Delta t s_{j+\frac{1}{2}}^{n+1}) = \frac{u_{j+\frac{1}{2}}^+ - u_{j+\frac{1}{2}}^-}{a_{j+\frac{1}{2}}^+ - a_{j+\frac{1}{2}}^-}$$

and the resulting numerical flux is

$$H_{j+\frac{1}{2}}(t) := \frac{a_{j+\frac{1}{2}}^+ f(u_{j+\frac{1}{2}}^-) - a_{j+\frac{1}{2}}^- f(u_{j+\frac{1}{2}}^+)}{a_{j+\frac{1}{2}}^+ - a_{j+\frac{1}{2}}^-} + \frac{a_{j+\frac{1}{2}}^+ a_{j+\frac{1}{2}}^-}{2} \left[\frac{u_{j+\frac{1}{2}}^+ - u_{j+\frac{1}{2}}^-}{a_{j+\frac{1}{2}}^+ - a_{j+\frac{1}{2}}^-} \right]. \quad (2.11)$$

2.2. Modified CU2[4]. We approximate the values of the solution at time level $t = t^{n+1}$ at the points $x_{j+\frac{1}{2},l}^n$ and $x_{j+\frac{1}{2},r}^n$, which are denoted by

$$u_{j+\frac{1}{2},l}^{n+1} = u_{j+\frac{1}{2},l}^n - \Delta t f(u_{j+\frac{1}{2},l}^n)_x, \quad u_{j+\frac{1}{2},r}^{n+1} = u_{j+\frac{1}{2},r}^n - \Delta t f(u_{j+\frac{1}{2},r}^n)_x.$$

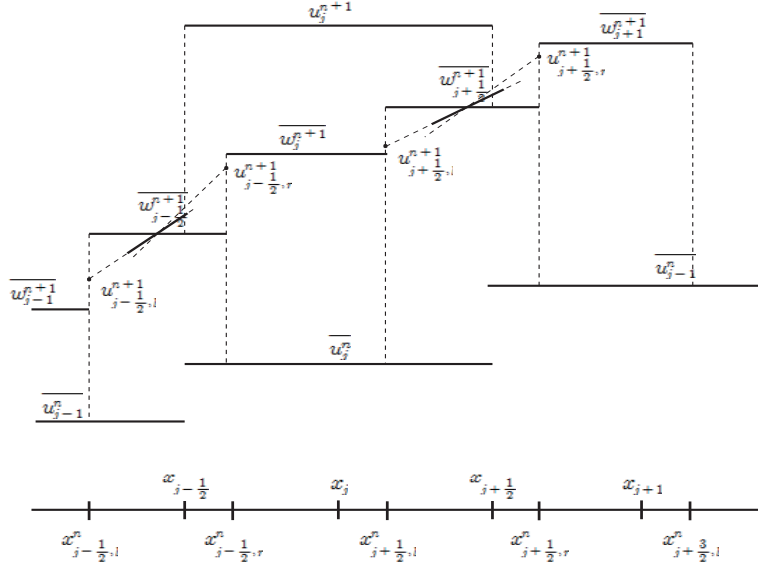


FIGURE 2. Modified CU2

Let $u_{j+\frac{1}{2},l}^{n+1} := \bar{w}_j^{n+1}$ and $u_{j+\frac{1}{2},r}^{n+1} := \bar{w}_{j+1}^{n+1}$. Then we apply the minmod limiter to these points and the slope $s_{j+\frac{1}{2}}^{n+1}$ is computed by

$$s_{j+\frac{1}{2}}^{n+1} = \text{minmod}\left(\frac{\bar{\omega}_{j+\frac{1}{2}}^{n+1} - u_{j+\frac{1}{2},l}^{n+1}}{\delta}, \frac{u_{j+\frac{1}{2},r}^{n+1} - \bar{\omega}_{j+\frac{1}{2}}^{n+1}}{\delta}\right) \quad (2.12)$$

where $\delta := \frac{\Delta t}{2}(a_{j+\frac{1}{2}}^+ - a_{j+\frac{1}{2}}^-)$ is equal to the length of the interval $[x_{j+\frac{1}{2},l}^n, x_{j+\frac{1}{2},r}^n]$. Figure 2 shows that how we can compute slope using (12). In Figure 2, the slope $s_{j+\frac{1}{2}}^{n+1}$ of Modified CU2 is the smaller one from two slopes which computed by connecting $u_{j+\frac{1}{2},l}^{n+1}$ with middle point of $\bar{w}_{j+\frac{1}{2}}^{n+1}$ and connecting $u_{j+\frac{1}{2},r}^{n+1}$ with middle point of $\bar{w}_{j+\frac{1}{2}}^{n+1}$. Consequently, Modified CU2 is less dissipative than Modified CU1. Then the resulting numerical flux is

$$H_{j+\frac{1}{2}}(t) := \frac{a_{j+\frac{1}{2}}^+ f(u_{j+\frac{1}{2}}^-) - a_{j+\frac{1}{2}}^- f(u_{j+\frac{1}{2}}^+)}{a_{j+\frac{1}{2}}^+ - a_{j+\frac{1}{2}}^-} + a_{j+\frac{1}{2}}^+ a_{j+\frac{1}{2}}^- \left[\frac{u_{j+\frac{1}{2}}^+ - u_{j+\frac{1}{2}}^-}{a_{j+\frac{1}{2}}^+ - a_{j+\frac{1}{2}}^-} - q_{j+\frac{1}{2}} \right]. \quad (2.13)$$

We will refer to $q_{j+\frac{1}{2}}$ that called the anti-diffusion,

$$q_{j+\frac{1}{2}} = \frac{1}{2} \lim_{\Delta t \rightarrow 0} \{\Delta t s_{j+\frac{1}{2}}^{n+1}\} = \text{minmod}\left(\frac{u_{j+\frac{1}{2}}^+ - \omega_{j+\frac{1}{2}}^{int}}{a_{j+\frac{1}{2}}^+ - a_{j+\frac{1}{2}}^-}, \frac{\omega_{j+\frac{1}{2}}^{int} - u_{j+\frac{1}{2}}^-}{a_{j+\frac{1}{2}}^+ - a_{j+\frac{1}{2}}^-}\right),$$

where the intermediate value :

$$\omega_{j+\frac{1}{2}}^{int} = \lim_{\Delta t \rightarrow 0} \bar{\omega}_{j+\frac{1}{2}}^{n+1} = \frac{a_{j+\frac{1}{2}}^+ u_{j+\frac{1}{2}}^+ - a_{j+\frac{1}{2}}^- u_{j+\frac{1}{2}}^- - \{f(u_{j+\frac{1}{2}}^+) - f(u_{j+\frac{1}{2}}^-)\}}{a_{j+\frac{1}{2}}^+ - a_{j+\frac{1}{2}}^-}.$$

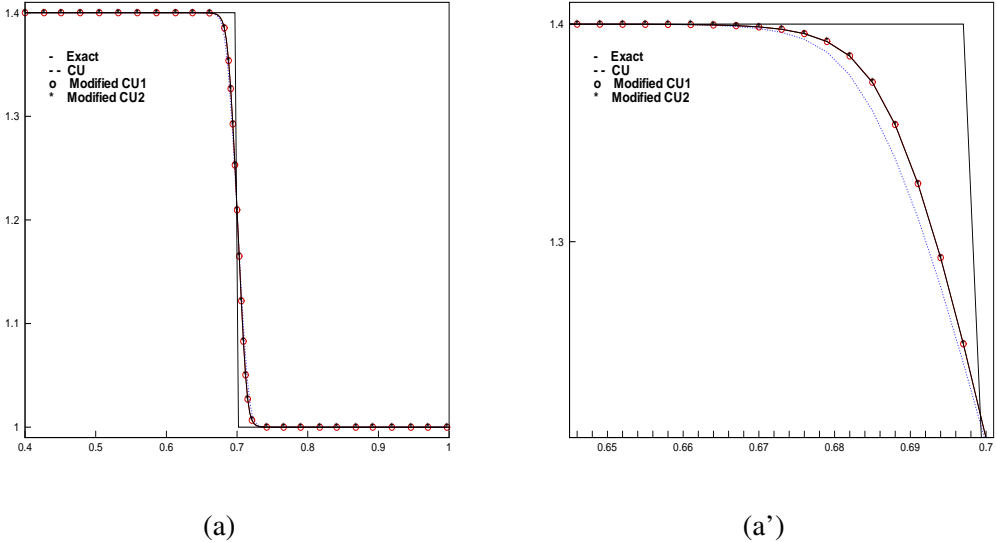


FIGURE 3. Moving contact discontinuity: (a) Numerical solution of density at $T = 2.0$. (a') Zoom.

3. NUMERICAL RESULTS FOR ONE DIMENSIONAL PROBLEM

We implement the idea of modified CU1 and modified CU2 to various problems. We consider Euler equation of gas dynamics for ideal gases:

$$\frac{\partial}{\partial t} \begin{bmatrix} \rho \\ m \\ E \end{bmatrix} + \frac{\partial}{\partial x} \begin{bmatrix} m \\ \rho u^2 + p \\ u(E + p) \end{bmatrix} = 0, \quad p = (\gamma - 1) \cdot (E - \frac{\rho}{2} u^2). \quad (3.1)$$

Here, $\rho, u, m = \rho u$, p and E are density, velocity, momentum, pressure and the total energy, respectively.

Example 1. Moving contact wave. We consider the 1-D Riemann problem(moving contact wave) for Euler equation on the interval $[0.4, 1]$ with the initial data :

$$(\rho, u, p) = \begin{cases} (1.4, 0.1, 1), & x < 0.5, \\ (1, 0.1, 1), & x > 0.5. \end{cases} \quad (3.2)$$

For this example, CFL is 0.475 and the number of grid N is 200. Figure 3 shows the numerical solution at time $T = 2.0$ by semi-discrete central upwind scheme(CU), Modified CU1, Modified CU2 and exact solution. The results are shown in Figure 3, where one can clearly see that Modified CU1 and Modified CU2 achieve a better resolution than CU.

Example 2. Steady contact discontinuity. We consider the 1-D Riemann problem(steady contact discontinuity) for Euler equation on the interval $[-0.2, 0.2]$ with the initial data :

$$(\rho, u, p) = \begin{cases} u_L = (1, 0, 2.5), & x < 0, \\ u_R = (0.5, 0, 2.5), & x > 0. \end{cases} \quad (3.3)$$

For this example, CFL is 0.5 and N is 200. Figure 4 shows the numerical solution of density at time $T = 10.0$ by CU, Modified CU1, Modified CU2 and exact solution. It clearly illustrates the advantage of the Modified CU1 and Modified CU2 in this example.

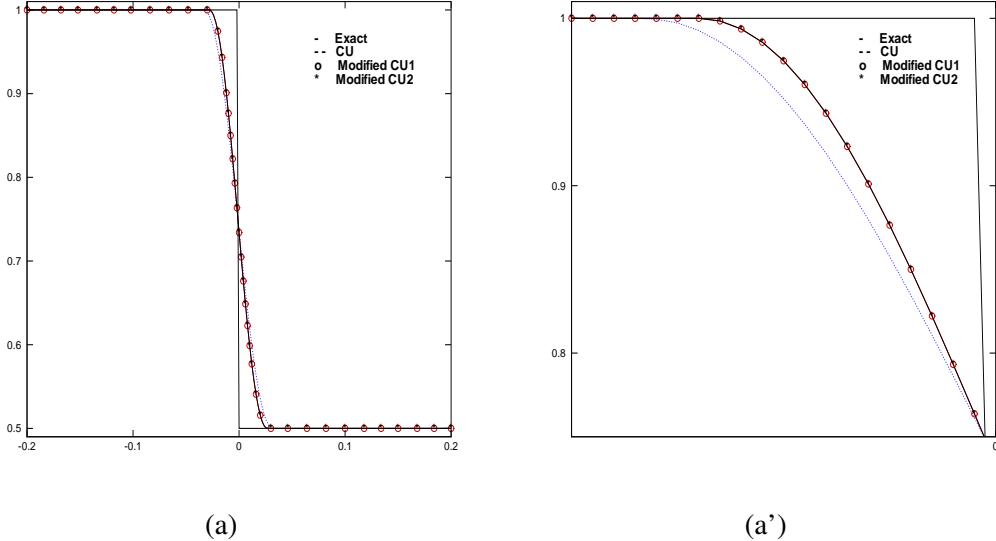


FIGURE 4. Steady contact discontinuity: (a) Numerical solution of density at $T = 10.0$. (a') Zoom.

Example 3. Sod's shock tube. We consider the 1-D Riemann problem(Sod's shock tube) for Euler equation on the interval $[0,1]$ with the initial data [1]:

$$(\rho, u, p) = \begin{cases} (1.0, 0.0, 1.0), & x < 0.5, \\ (0.125, 0.0, 0.1), & x > 0.5. \end{cases} \quad (3.4)$$

For this example, CFL is 0.5 and N is 100. Figure 5 (a)-(d) show the numerical solution of density at time $T = 0.2531$ by CU, Modified CU1, Modified CU2 and exact solution. Modified

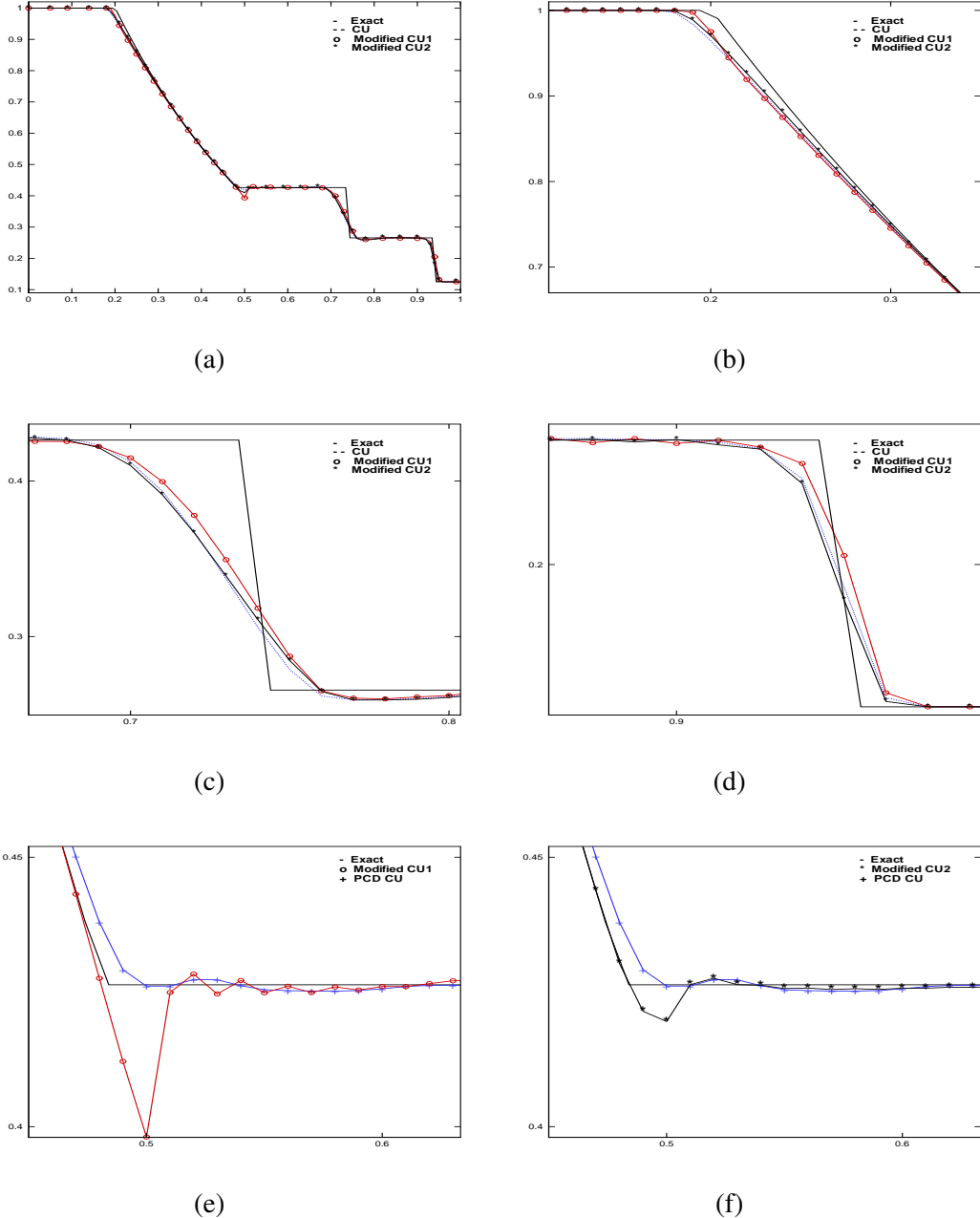


FIGURE 5. Sod's shock tube: Numerical solution of density at $T = 0.2531$, (a) CU, Modified CU1 and Modified CU2, (b), (c) and (d) Zooms, (e) Comparison of Modified CU1 and PCD CU (Zoom near expansion region), (f) Comparison of Modified CU2 and PCD CU (Zoom near expansion region)

CU1 shows the best result, however we can see that Modified CU1 has some oscillation near the expansion. To decrease the oscillation, we apply partial characteristic decomposition(PCODE CU) done by Kurganov and Petrova [6]. The numerical result given in Figure 5 (e) show that unnecessary oscillation by Modified CU1 is greatly reduced by applying partial characteristic decomposition. Modified CU2 and PCD CU are compared in Figure 5 (f). The result shows PCD CU has a better resolution than Modified CU2 near expansion.

Example 4. Acoustic wave. We consider the 1-D Riemann problem(Acoustic wave) for Euler equation on the interval $[-5,5]$ with the initial data[1]:

$$(\rho, u, p) = \begin{cases} (3.857143, 2.629369, 10.333333), & x < -4.0, \\ (1 + 0.2 \cdot \sin(5x), 0, 1), & x > -4.0. \end{cases} \quad (3.5)$$

For this example, CFL is 0.5 and N is 400. Figure 6 shows the numerical solution of density at time $T = 1.8$ by CU, Modified CU1 and Modified CU2. Fine grid reference solution is obtained by CU with $\Delta x = 1/2000$. The results are shown in Figure 6, where one can clearly see that Modified CU2 achieves a better resolution than CU and Modified CU1.

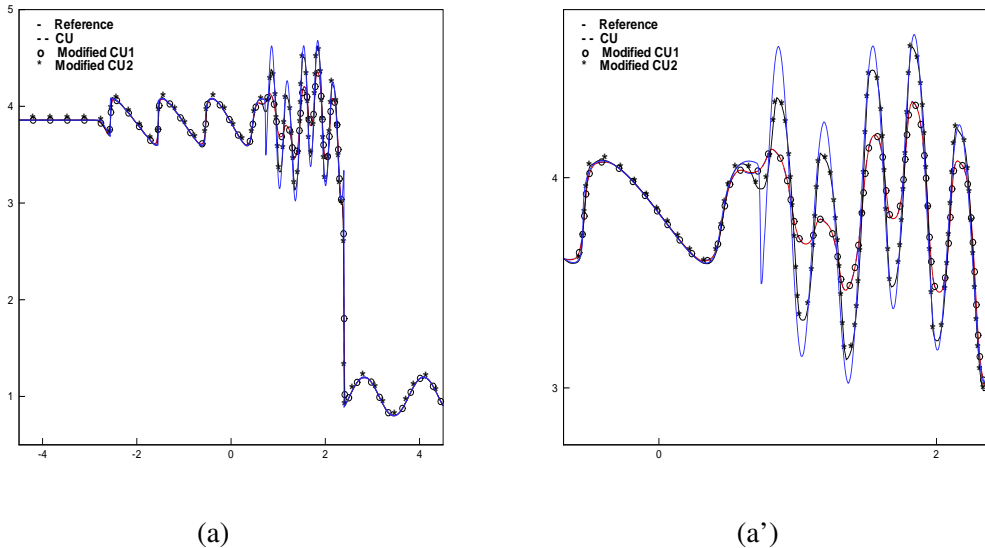


FIGURE 6. Acoustic wave: (a) Numerical solution of density at $T = 1.8$. (a') Zoom.

Example 5. Woodward-Colella problem. We consider the 1-D Riemann problem(Woodward-Colella problem) for Euler equation on the interval $[0,1]$ with the initial data :

$$(\rho, u, p) = \begin{cases} u_L = (1, 0, 2500), & 0 \leq x < 0.1, \\ u_M = (1, 0, 0.025), & 0.1 \leq x < 0.9, \\ u_R = (1, 0, 250), & 0.9 \leq x < 1. \end{cases} \quad (3.6)$$

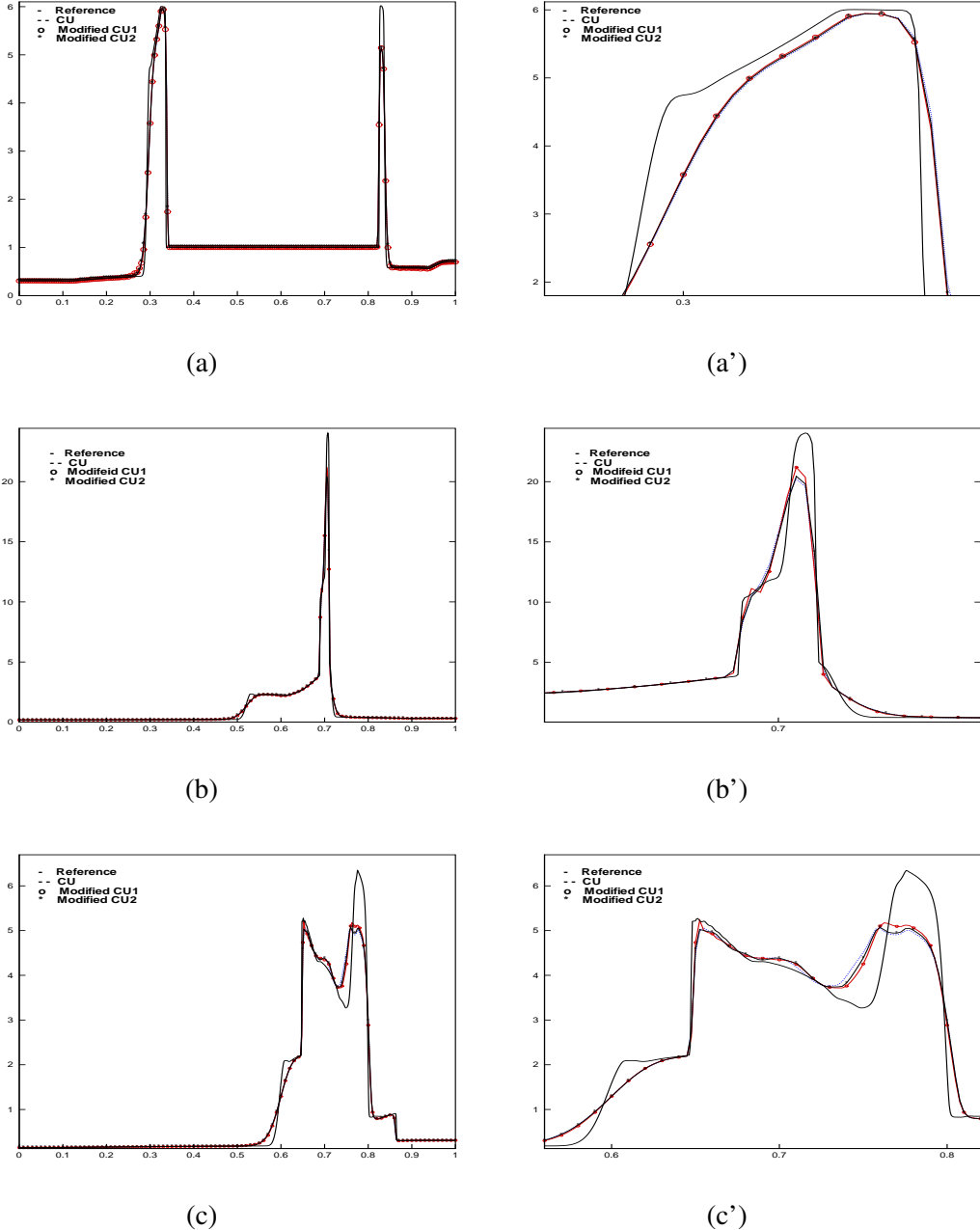


FIGURE 7. Woodward-Colella problem: (a), (b), (c) Numerical solution of density at $T = 0.01, 0.03$, and 0.038 , respectively. (a'), (b') and (c') Zooms at the corresponding times.

For this example, CFL is 0.475 and N is 400. Figure 7 shows the numerical solution of density at time $T = 0.01, 0.03$ and 0.038 by CU, Modified CU1 and Modified CU2. A reference solution is computed by CU scheme with 1600 grid points. The results are shown in Figure 7 where one can see that Modified CU1 and Modified CU2 achieve a better resolution than CU.

4. TWO DIMENSIONAL SEMI-DISCRETE CENTRAL UPWIND SCHEME

In this section, we consider semi-discrete central upwind scheme [4] for two dimensional system of hyperbolic conservation laws:

$$u_t + f(u)_x + g(u)_y = 0. \quad (4.1)$$

We consider uniform grids: $x_\alpha := \alpha\Delta x$, $y_\beta := \beta\Delta y$, $\Delta t := t^{n+1} - t^n$ and at a certain time level cell average of the solution:

$$\tilde{u}(x, y, t^n) = \sum_{j,k} [\bar{u}_{j,k}^n + (u_x)_{j,k}^n(x - x_j) + (u_y)_{j,k}^n(y - y_k)] \chi_{j,k}(x, y) \quad (4.2)$$

is also available. $\chi_{j,k}(x, y)$ is the characteristic function over the cell $(x_{j-\frac{1}{2}}, x_{j+\frac{1}{2}}) \times (y_{k-\frac{1}{2}}, y_{k+\frac{1}{2}})$ and $(u_x)_{j,k}^n$ and $(u_y)_{j,k}^n$ stand for an approximation of the x- and y-derivatives of u at the cell centers (x_j, y_k) at time $t = t^n$. We take

$$\begin{aligned} (u_x)_{j,k}^n &= \text{minmod}\left(\theta \frac{\bar{u}_{j+1,k}^n - \bar{u}_{j,k}^n}{\Delta x}, \frac{\bar{u}_{j+1,k}^n - \bar{u}_{j-1,k}^n}{2\Delta x}, \theta \frac{\bar{u}_{j,k}^n - \bar{u}_{j-1,k}^n}{\Delta x}\right), \theta \in [1, 2] \\ (u_y)_{j,k}^n &= \text{minmod}\left(\theta \frac{\bar{u}_{j,k+1}^n - \bar{u}_{j,k}^n}{\Delta y}, \frac{\bar{u}_{j,k+1}^n - \bar{u}_{j,k-1}^n}{2\Delta y}, \theta \frac{\bar{u}_{j,k}^n - \bar{u}_{j,k-1}^n}{\Delta y}\right). \end{aligned} \quad (4.3)$$

In the case of convex fluxes f and g , the local speeds can be estimated as follow:

$$\begin{aligned} a_{j+\frac{1}{2},k}^+ &:= \max\{\lambda_N(A(u_{j+1,k}^W)), \lambda_N(A(u_{j,k}^E)), 0\}, \\ b_{j,k+\frac{1}{2}}^+ &:= \max\{\lambda_N(B(u_{j,k+1}^S)), \lambda_N(B(u_{j,k}^N)), 0\}, \\ a_{j+\frac{1}{2},k}^- &:= \min\{\lambda_1(A(u_{j+1,k}^W)), \lambda_1(A(u_{j,k}^E)), 0\}, \\ b_{j,k+\frac{1}{2}}^- &:= \min\{\lambda_1(B(u_{j,k+1}^S)), \lambda_1(B(u_{j,k}^N)), 0\}. \end{aligned} \quad (4.4)$$

Here, $\lambda_1 < \lambda_2 < \dots < \lambda_N$ are N eigenvalues of the corresponding Jacobian matrix, $A := \frac{\partial f}{\partial u}$ and $B := \frac{\partial g}{\partial u}$, and the point values of (23) are given by:

$$\begin{aligned} u_{j,k}^E &:= \bar{u}_{j,k}^n + \frac{\Delta x}{2}(u_x)_{j,k}^n, & u_{j,k}^N &:= \bar{u}_{j,k}^n + \frac{\Delta y}{2}(u_y)_{j,k}^n, \\ u_{j,k}^W &:= \bar{u}_{j,k}^n - \frac{\Delta x}{2}(u_x)_{j,k}^n, & u_{j,k}^S &:= \bar{u}_{j,k}^n - \frac{\Delta y}{2}(u_y)_{j,k}^n. \end{aligned}$$

A second order two dimensional semi-discrete central-upwind scheme can be obtained in the following flux form:

$$\frac{d}{dt} \bar{u}_{j,k}(t) = -\frac{H_{j+\frac{1}{2},k}^x(t) - H_{j-\frac{1}{2},k}^x(t)}{\Delta x} - \frac{H_{j,k+\frac{1}{2}}^y(t) - H_{j,k-\frac{1}{2}}^y(t)}{\Delta y}.$$

4.1. Modified CU1. The second-order numerical fluxes are:

$$H_{j+\frac{1}{2},k}^x(t) := \frac{a_{j+\frac{1}{2},k}^+ f(u_{j,k}^E) - a_{j+\frac{1}{2},k}^- f(u_{j+1,k}^W)}{a_{j+\frac{1}{2},k}^+ - a_{j+\frac{1}{2},k}^-} + \frac{a_{j+\frac{1}{2},k}^+ a_{j+\frac{1}{2},k}^-}{2} \left[\frac{u_{j+1,k}^W - u_{j,k}^E}{a_{j+\frac{1}{2},k}^+ - a_{j+\frac{1}{2},k}^-} \right],$$

$$H_{j,k+\frac{1}{2}}^y(t) := \frac{b_{j,k+\frac{1}{2}}^+ g(u_{j,k}^N) - b_{j,k+\frac{1}{2}}^- g(u_{j,k+1}^S)}{b_{j,k+\frac{1}{2}}^+ - b_{j,k+\frac{1}{2}}^-} + \frac{b_{j,k+\frac{1}{2}}^+ b_{j,k+\frac{1}{2}}^-}{2} \left[\frac{u_{j,k+1}^S - u_{j,k}^N}{b_{j,k+\frac{1}{2}}^+ - b_{j,k+\frac{1}{2}}^-} \right].$$

4.2. Modified CU2[4]. The second-order numerical fluxes are:

$$H_{j+\frac{1}{2},k}^x(t) := \frac{a_{j+\frac{1}{2},k}^+ f(u_{j,k}^E) - a_{j+\frac{1}{2},k}^- f(u_{j+1,k}^W)}{a_{j+\frac{1}{2},k}^+ - a_{j+\frac{1}{2},k}^-} + a_{j+\frac{1}{2},k}^+ a_{j+\frac{1}{2},k}^- \left[\frac{u_{j+1,k}^W - u_{j,k}^E}{a_{j+\frac{1}{2},k}^+ - a_{j+\frac{1}{2},k}^-} - q_{j+\frac{1}{2},k}^x \right],$$

$$H_{j,k+\frac{1}{2}}^y(t) := \frac{b_{j,k+\frac{1}{2}}^+ g(u_{j,k}^N) - b_{j,k+\frac{1}{2}}^- g(u_{j,k+1}^S)}{b_{j,k+\frac{1}{2}}^+ - b_{j,k+\frac{1}{2}}^-} + b_{j,k+\frac{1}{2}}^+ b_{j,k+\frac{1}{2}}^- \left[\frac{u_{j,k+1}^S - u_{j,k}^N}{b_{j,k+\frac{1}{2}}^+ - b_{j,k+\frac{1}{2}}^-} - q_{j,k+\frac{1}{2}}^y \right].$$

Similarly to the one-dimensional case, we will build in anti-diffusion term. They are given by:

$$q_{j+\frac{1}{2},k}^x = \text{minmod} \left(\frac{u_{j+1,k}^{NW} - \omega_{j+\frac{1}{2},k}^{int}}{a_{j+\frac{1}{2},k}^+ - a_{j+\frac{1}{2},k}^-}, \frac{u_{j+1,k}^{SW} - \omega_{j+\frac{1}{2},k}^{int}}{a_{j+\frac{1}{2},k}^+ - a_{j+\frac{1}{2},k}^-}, \frac{\omega_{j+\frac{1}{2},k}^{int} - u_{j,k}^{NE}}{a_{j+\frac{1}{2},k}^+ - a_{j+\frac{1}{2},k}^-}, \frac{\omega_{j+\frac{1}{2},k}^{int} - u_{j,k}^{SE}}{a_{j+\frac{1}{2},k}^+ - a_{j+\frac{1}{2},k}^-} \right),$$

$$q_{j,k+\frac{1}{2}}^y = \text{minmod} \left(\frac{u_{j,k+1}^{SW} - \omega_{j,k+\frac{1}{2}}^{int}}{b_{j,k+\frac{1}{2}}^+ - b_{j,k+\frac{1}{2}}^-}, \frac{u_{j,k+1}^{SE} - \omega_{j,k+\frac{1}{2}}^{int}}{b_{j,k+\frac{1}{2}}^+ - b_{j,k+\frac{1}{2}}^-}, \frac{\omega_{j,k+\frac{1}{2}}^{int} - u_{j,k}^{NW}}{b_{j,k+\frac{1}{2}}^+ - b_{j,k+\frac{1}{2}}^-}, \frac{\omega_{j,k+\frac{1}{2}}^{int} - u_{j,k}^{NE}}{b_{j,k+\frac{1}{2}}^+ - b_{j,k+\frac{1}{2}}^-} \right),$$

where the intermediate values are:

$$\omega_{j+\frac{1}{2},k}^{int} = \frac{a_{j+\frac{1}{2},k}^+ u_{j+1,k}^W - a_{j+\frac{1}{2},k}^- u_{j,k}^E - \{f(u_{j+1,k}^W) - f(u_{j,k}^E)\}}{a_{j+\frac{1}{2},k}^+ - a_{j+\frac{1}{2},k}^-},$$

$$\omega_{j,k+\frac{1}{2}}^{int} = \frac{b_{j,k+\frac{1}{2}}^+ u_{j,k+1}^S - b_{j,k+\frac{1}{2}}^- u_{j,k}^N - \{g(u_{j,k+1}^S) - g(u_{j,k}^N)\}}{b_{j,k+\frac{1}{2}}^+ - b_{j,k+\frac{1}{2}}^-},$$

and $u_{j,k}^{NE}$, $u_{j,k}^{NW}$, $u_{j,k}^{SE}$ and $u_{j,k}^{SW}$ are the corresponding corner point values of the piecewise linear reconstruction (21) in the (j, k) th cell:

$$\begin{aligned} u_{j,k}^{NE} &:= \bar{u}_{j,k}^n + \frac{\Delta x}{2}(u_x)_{j,k}^n + \frac{\Delta y}{2}(u_y)_{j,k}^n, & u_{j,k}^{NW} &:= \bar{u}_{j,k}^n - \frac{\Delta x}{2}(u_x)_{j,k}^n + \frac{\Delta y}{2}(u_y)_{j,k}^n, \\ u_{j,k}^{SE} &:= \bar{u}_{j,k}^n + \frac{\Delta x}{2}(u_x)_{j,k}^n - \frac{\Delta y}{2}(u_y)_{j,k}^n, & u_{j,k}^{SW} &:= \bar{u}_{j,k}^n - \frac{\Delta x}{2}(u_x)_{j,k}^n - \frac{\Delta y}{2}(u_y)_{j,k}^n. \end{aligned}$$

5. NUMERICAL RESULTS FOR TWO DIMENSIONAL PROBLEM

We apply these methods to 2-D Euler equation of gas dynamics for ideal gases:

$$\frac{\partial}{\partial t} \begin{bmatrix} \rho \\ \rho u \\ \rho v \\ E \end{bmatrix} + \frac{\partial}{\partial x} \begin{bmatrix} \rho u \\ \rho u^2 + p \\ \rho u v \\ u(E + p) \end{bmatrix} + \frac{\partial}{\partial y} \begin{bmatrix} \rho v \\ \rho u v \\ \rho v^2 + p \\ v(E + p) \end{bmatrix} = 0, \quad p = (\gamma - 1) \cdot [(E - \frac{\rho}{2}(u^2 + v^2)]. \quad (5.1)$$

Here, ρ , u , v , p and E are the density, the x -velocity and the y -velocity, the pressure and the total energy, respectively.

Example 6. 2-D Contact discontinuity. We consider the 2-D Riemann problem for Euler equation on the interval $[0,1] \times [0,1]$, with the initial data :

$$\begin{cases} (p_1, \rho_1, u_1, v_1) &= (1.1, 1.1, 0, 0) \\ (p_2, \rho_2, u_2, v_2) &= (0.35, 0.5065, 0.8939, 0) \\ (p_3, \rho_3, u_3, v_3) &= (1.1, 1.1, 0.8939, 0.8939) \\ (p_4, \rho_4, u_4, v_4) &= (0.35, 0.5065, 0, 0.8939) \end{cases}$$

For this example, CFL is 0.05. Figures 8 and 9 show the numerical solution at time $T = 0.3$ by CU, Modified CU1 and Modified CU2 with $N \times N = 400 \times 400$ and 1600×1600 , respectively. Modified CU1 and Modified CU2 have a better resolution than CU. In Figure 9 which has the finer mesh of 1600×1600 , the center region is more clearly resolved in case of Modified CU1 and Modified CU2 compared CU. This shows less numerical dissipation for Modified CU1 and Modified CU2 than CU.

Concluding remark. For moving contact wave and steady contact discontinuity examples, Modified CU1 and Modified CU2 performs similar and have a better resolution than CU. For Sod's shock tube problem, Modified CU1 achieves a better resolution than Modified CU2 and CU but Modified CU1 generates oscillation. By applying the partial characteristic decomposition(PCD CU), this oscillation is successfully removed. PCD CU also has a better resolution than Modified CU1 near expansion. On the other hand, Modified CU2 has a better resolution than Modified CU1 and CU for acoustic wave. In case of Woodward-Colella problem, Modified CU1 and Modified CU2 have a better resolution than CU. For 2-D Riemann problem of Euler equation, Modified CU1 and Modified CU2 also have a better resolution than CU. This is more apparent for finer grids.

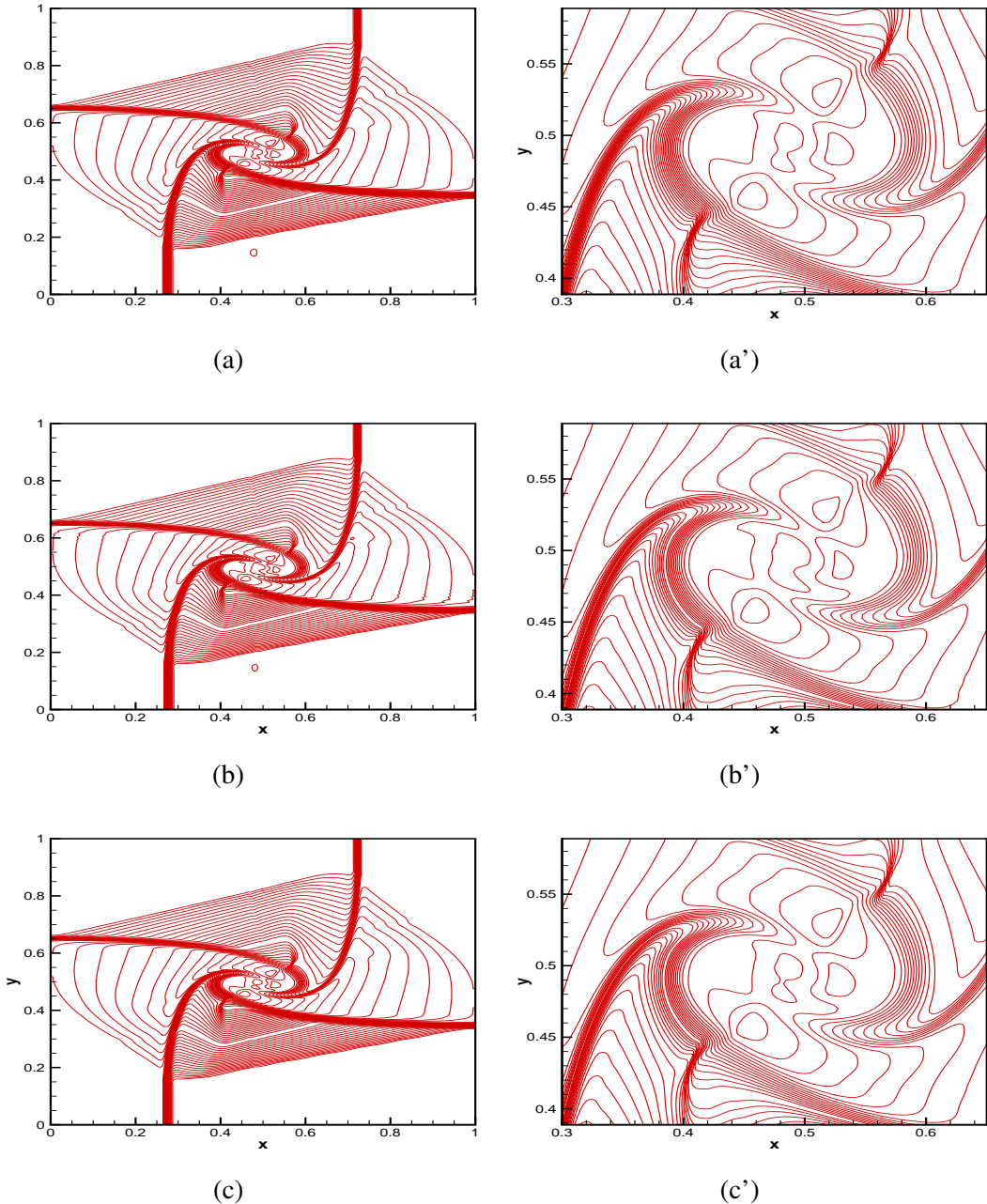


FIGURE 8. 2-D contact discontinuity: Numerical solution of density at $T = 0.3$ by 400×400 , (a) CU, (b) Modified CU1, (c) Modified CU2. (a'), (b') and (c') Corresponding zooms.

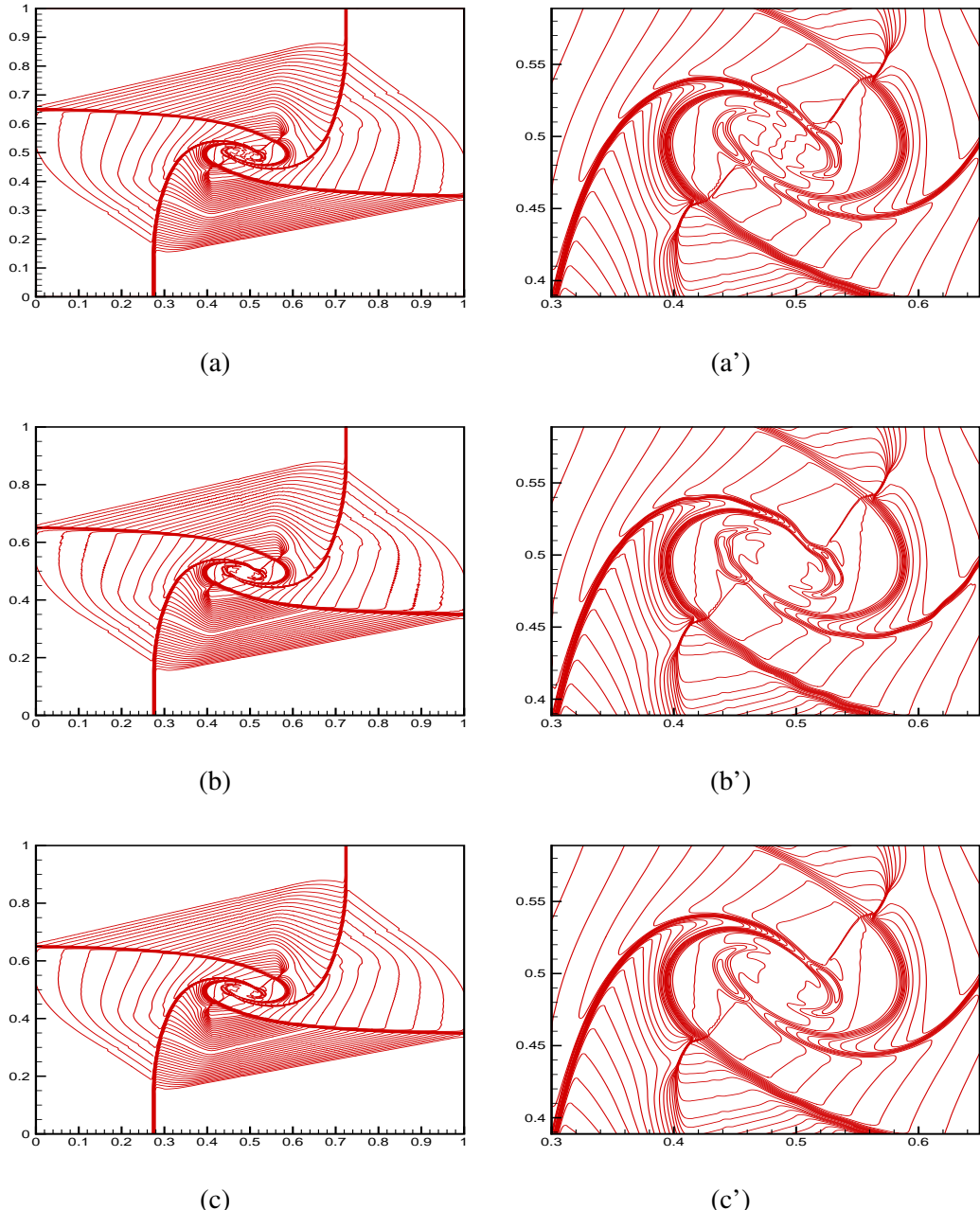


FIGURE 9. 2-D contact discontinuity: Numerical solution of density at $T = 0.3$ by 1600×1600 , (a) CU, (b) Modified CU1, (c) Modified CU2. (a'), (b') and (c') Corresponding zooms.

ACKNOWLEDGMENTS

We would like to thank anonymous referee for valuable comments and corrections.

REFERENCES

- [1] B. Einfeldt, *On godunov-type methods for gas dynamics*, J. Numer. Anal. vol. 25 No. 2, 1988.
- [2] G. S. Jiang and E. Tadmor, *Nonoscillatory central schemes for multidimensional hyperbolic conservation laws*, SIAM J. Sci. Comput., 19, 1998, pp. 1832-1917.
- [3] S. Karni, A. Kurganov and G. Petrova, *A smoothness indicator for adaptive algorithms for hyperbolic systems*, J. Comput. Phys. 178, 2002, pp. 323-341.
- [4] A. Kurganov and C. T. Lin, *On the Reduction of Numerical Dissipation in Central-Upwind Schemes*, Commun. Comput. Phys. Vol. 2, 2007, pp. 141-163.
- [5] A. Kurganov, S. Noelle and G. Petrova, *Semi-discrete central-upwind scheme for hyperbolic conservation laws and Hamilton-Jacobi equation*, SIAM J. Sci. Comput. 23, 2001, pp. 707-740.
- [6] A. Kurganov and G. Petrova, *Central schemes and contact discontinuities*, Math. Model. Numer. Anal. 34, 2000, pp. 1259-1275.
- [7] A. Kurganov, G. Petrova and B. Popov, *Adaptive semi-discrete central-upwind schemes for nonconvex hyperbolic conservation law*, SIAM. J. Sci. Comput. Vol 29, No. 6, 2007, pp. 2381-2401.
- [8] A. Kurganov and E. Tadmor, *New high-resolution central schemes for nonlinear conservation laws and convection-diffusion equations*, J. Comput. Phys. 160, 2000, pp. 241-282.
- [9] P.D. Lax, *Weak solutions of nonlinear hyperbolic equations and their numerical computation*, Comm. Pure Appl. Math. 1954, pp. 159-193.
- [10] K. A. Lie and S. Noelle, *On the artificial compression method for second-order nonoscillatory central difference schemes for systems of conservation laws*, SIAM J. Sci. Comput. 24, 2003, pp. 1157-1174.
- [11] X. D. Liu and E. Tadmor, *Third order nonoscillatory central scheme for hyperbolic conservation laws*, Numer. Math. vol. 79, 1988, pp. 397-425.
- [12] H. Nessyahu and E. Tadmor, *Non-oscillatory central differencing for hyperbolic conservation laws*, J. Comput. Phys. 87, 1990, pp. 408-463.
- [13] S. Shin and W. Hwang, *Central schemes with Lax-Wendroff type time discretizations*, Bull. Korean Math. Soc. No. 4, 2011, pp. 873-896.